Statistical model of radiation damage within an atomic cluster irradiated by photons from free-electron-laser.

B. Ziaja [*,†], E. Weckert [*] and T. Möller [‡]

[*] *HASYLAB at DESY, Notkestr. 85, D-22603 Hamburg, Germany*

[†] *Department of Theoretical Physics, Institute of Nuclear Physics, Radzikowskiego 152, 31-342 Cracow, Poland*

[‡] *Technische Universität Berlin, Institut für Atomare Physik und Fachdidaktik, 10623 Berlin, Hardenbergstrasse 36, Germany*

20 January 2007

Corresponding author:
Beata Ziaja,
HASYLAB at DESY, Notkestr. 85,
D-22603 Hamburg, Germany,
E-mail: ziaja@mail.desy.de,
Telephone number: +49-40-89984506

Short title: Radiation damage in FEL irradiated samples.

Number of pages:16 , **Number of tables:0** , **Number of figures:4**

Title: **Statistical model of radiation damage within an atomic cluster irradiated by photons from free-electron-laser (FEL).**

Abstract: Here we report on the present status of our project on statistical modelling of charge dynamics within irradiated samples. Boltzmann statistical approach to model the radiation damage in samples irradiated by FEL photons is tested in a study case of a spherically symmetric xenon cluster. Qualitative agreement between the model predictions and the experimental data is found. The results obtained demonstrate the potential of the statistical method for describing the non-equilibrium dynamics of samples exposed to FEL radiation.

Keywords: free-electron lasers, radiation damage, computer simulations

1 Introduction

Free-electron-lasers (FELs) open new horizons in studying the structure of matter. It is expected that the intense radiation from the FELs, emitted in pulses of ultrashort duration [LCLS, 2000, DESY, 2001, DESY, 2006, SCSS, 2006, Dattoli et al., 2005]. may probe dynamic states of matter, transitions and reactions happening within tens of femtoseconds, and also generate extreme states of matter [Lee at el., 2002]. The X-ray FEL (XFEL) promises significant progress in structural studies of biological systems, especially in studies of non-repetitive samples. Low radiation tolerance of these samples prevents an accurate determination of their structure in standard diffraction experiments. The recent studies of the progress of the damage formation [Neutze et al., 2000, Jurek et al., 2004, Hau-Riege et al., 2004] indicate that the radiation tolerance might be extended at ultrafast imaging with high radiation doses.

For this and other potential applications of FELs, we need a detailed understanding of how the intense radiation of short wavelengths interacts with matter. The radiation damage of samples irradiated by soft X-rays differs considerably from that induced by high power IR-lasers [Kanapathipillai, 2006]. In the latter case plasma heating by inverse bremsstrahlung (IB) is the dominant damage process at moderate intensities [Ditmire et al., 1996],
[Last & Jortner, 1999, Krainov & Smirnov, 2002]. For FELs, at different energies of the FEL photons different processes are contributing to the radiation damage. At VUV photon energies the inverse bremsstrahlung process is believed to deliver most of the energy needed for the efficient ionization of an irradiated system [Santra & Greene, 2003],
[Meyer-ter-Vehn et al., 2004, Krenz & J. Meyer-ter-Vehn, 2005, Fisher et al., 2006]. Photons of shorter wavelengths may excite electrons from inner shells of atoms, creating core holes [Saalmann & Rost, 2002]. Photoemissions, core-hole creations and subsequent Auger emissions of secondary electrons contribute to the radiation damage that then affects not only the sample but also the optical elements of the FEL beamline.

Radiation damage by photons from the VUV FEL is now under intense experimental and theoretical investigation. The large number of VUV photons absorbed per atom that was observed during the first experiments at DESY [Wabnitz et al., 2002, Wabnitz, 2003] could not be explained using the well-established standard calculations for photon absorption
[Santra & Greene, 2003, Wabnitz et al., 2002, Wabnitz, 2003]. This indicated that the ionization of samples irradiated by energetic photons progresses in a different way than that observed in the optical energy range. These surprising results stimulated intense theoretical effort. Several interesting models have been proposed
[Santra & Greene, 2003, Siedschlag & Rost, 2004, Bauer, 2004, Jungreuthmayer et al., 2005],

which could explain various aspects of the increased photoabsorption and ionization dynamics observed in the experiments (for review see [Saalmann et al., 2006]). On the other hand, there are still some controversies, e. g. regarding the role of the inverse bremsstrahlung mechanism, screening effects and of the inner ionization processes in the ionization dynamics. Statistical model of radiation damage, computationally efficient also for large and spatially non-uniform samples, could be useful in evaluating the contributions of different mechanisms to the overall ionization dynamics.

In [Ziaja et al., 2006] we proposed a statistical approach to describe the evolution of irradiated samples. This approach was based on the first-principles Boltzmann method. Boltzmann equations evolve classical electron and ion densities in phase space from their initial configurations. The full spatio-temporal characteristics of the electron and ion dynamics can be easily obtained with this transport method. As charge densities are directly evolved with Boltzmann equations, the averaged observables, O, of interest can then be calculated from their convolution with the charge densities obtained, $\langle O(t) \rangle = \int O(\mathbf{r}, \mathbf{v})\, \rho(\mathbf{r}, \mathbf{v}, t) d^3r\, d^3v$. These results are not biased with statistical errors.

The Boltzmann method is a promising alternative to the first-principles Monte Carlo (MC) or Molecular Dynamics (MD) methods which are commonly used [Neutze et al., 2000, Jurek et al., 2004, Heidenreich et al., 2005]. MC/MD algorithms become computationally inefficient if the number of particles, N, is large. In contrast, the efficiency of the simulation algorithm with the Boltzmann equations does not change directly with the number of particles in the sample, as the algorithm operates on smooth density functions. Therefore the efficiency of these algorithms depends only on the phase-space shape of the sample which is reflected in the number of grid points used in the simulation. Therefore Boltzmann approach can also work fine for large samples, where the MD/MC methods fail.

The applicability of Boltzmann equations is, however, limited to the systems which fulfill the assumptions of molecular chaos and two-body collisions. These assumptions are usually justified by a presence of short range forces [Sharkofsky et al., 1966],
[Chapman & Cowling, 1970]. The single particle density function obtained with Boltzmann equations does not contain any information on three-body and higher order correlations. If the higher order correlations are important, a more fundamental Liouville equation for the N-particle density function should be applied. The Liouville equation reduces to the collisionless Vlasov equation [Sharkofsky et al., 1966] in case of an uncorrelated system. Fokker-Planck equation [Sharkofsky et al., 1966] can be derived as a limiting form of the Liouville equation for long-range (e. g. Coulomb) forces. It was proven in Ref. [Sharkofsky et al., 1966] that a correct description of many body Coulomb interactions of plasma electrons and ions as that obtained with the dedicated Fokker-Planck equations can

be also obtained with the two-body Boltzmann collision term, assuming the Debye cutoff in the Rutherford scattering cross section. This simplification does not apply to the electron-electron interactions, where the interacting charged particles have identical masses, and the momentum transfer during their collisions cannot be neglected.

Another disadvantage of the Boltzmann approach is its numerical complexity. Boltzmann equations are complicated sets of nonlinear integro-differential equations where partial derivatives appear in both spatial and velocity coordinates, $\partial/\partial\mathbf{r}$, and $\partial/\partial\mathbf{v}$. Advanced numerical methods have then to be applied.

In what follows we will apply Boltzmann method for studies of the radiation damage in samples irradiated by FEL photons. We will use the angular moment expansion of the Boltzmann equations. This expansion was described in detail in [Ziaja et al., 2006]. We will solve Boltzmann equations numerically in a study case of a spherically symmetric xenon cluster irradiated by VUV FEL photons. The results obtained will be discussed in detail. Finally, our conclusions will be listed.

2 Boltzmann equations

In [Ziaja et al., 2006] we formulated the specific Boltzmann equations describing the transport of electrons, atoms and ions inside a sample irradiated with FEL photons. In these equations it is enough to consider two gases: the gas of light electrons of masses, m and charges, $-e$, and the gas of heavy atoms/ions of masses, M, and charges, ie. Photons need not to be treated as an independent gas component, as they only enter the equations as a flux term in the photoionization source term. The gases of electrons and atoms/ions are represented by the density functions: $\rho^{(e)}(\mathbf{r},\mathbf{v},t)$, $\rho^{(i)}(\mathbf{r},\mathbf{v},t)$, where i denotes the ion charge $i = 0, 1, \ldots, N_J$, and N_J is an arbitrary number, describing the maximal ion charge in the system. The general coupled Boltzmann equations for electrons and ions are:

$$\partial_t \rho^{(e)}(\mathbf{r},\mathbf{v},t) + \mathbf{v}\cdot\partial_{\mathbf{r}}\rho^{(e)}(\mathbf{r},\mathbf{v},t) + \frac{e}{m}\left(\mathbf{E}(\mathbf{r},t) + \mathbf{v}\times\mathbf{B}(\mathbf{r},t)\right)\cdot\partial_{\mathbf{v}}\rho^{(e)}(\mathbf{r},\mathbf{v},t) = \Omega^{(e)}(\rho^{(e)},\rho^{(i)},\mathbf{r},\mathbf{v},t), \quad (1)$$

for electrons, and

$$\partial_t \rho^{(i)}(\mathbf{r},\mathbf{v},t) + \mathbf{v}\cdot\partial_{\mathbf{r}}\rho^{(i)}(\mathbf{r},\mathbf{v},t) - \frac{ie}{M}\left(\mathbf{E}(\mathbf{r},t) + \mathbf{v}\times\mathbf{B}(\mathbf{r},t)\right)\cdot\partial_{\mathbf{v}}\rho^{(i)}(\mathbf{r},\mathbf{v},t) = \Omega^{(i)}(\rho^{(e)},\rho^{(i)},\mathbf{r},\mathbf{v},t), \quad (2)$$

for atoms/ions, where we included the total electromagnetic force $\mathbf{F}$, $\mathbf{F}(\mathbf{r},\mathbf{v},t) = q(\mathbf{E}(\mathbf{r},t) + \mathbf{v}\times\mathbf{B}(\mathbf{r},t))$, acting on electrons and ions positioned between $\mathbf{r}$ and $\mathbf{r}+\mathbf{dr}$, which have velocities in the range $(\mathbf{v}, \mathbf{v}+\mathbf{dv})$. The electric field, $\mathbf{E}$, and magnetic field, $\mathbf{B}$, have two components. The first component describes the interaction of charges with external radiation. The second component describes internal electromagnetic interaction between electrons and ions. This component is a non-local function of electron and ion densities.

Collision terms, $\Omega^{(e,i)}$, describe changes of the electron/ion densities of velocities $(\mathbf{v}, \mathbf{v}+\mathbf{dv})$ measured at the positions $(\mathbf{r}, \mathbf{r}+\mathbf{dr})$ with time. These changes are due to short-range processes, e. g. (i) creations of the secondary electrons and highly charged ions via photo- and collisional ionizations, (ii) elastic and inelastic collisions of electrons and ions, (iii) the inverse bremsstrahlung process, i. e. absorptions and emissions of photons by electrons during the elastic electron-ion collisions, (iv) recombination processes etc. Number of short-range processes involved in the sample dynamics depends on the wavelength of the laser radiation. If collision terms are neglected, Boltzmann equations, Eqs. (1), (2), reduce to the Vlasov equations [Sharkofsky et al., 1966, Kruer, 1988] describing the evolution of a collisionless plasma.

Initial configuration of Eqs. (1), (2) is given by a smooth atomic density function, $\rho^{(0)}(\mathbf{r}, \mathbf{v}, 0)$, which represents the sample at $t = 0$.

Below we list the assumptions of the primary transport model dedicated for studying the radiation damage in xenon clusters at VUV photon energies [Ziaja et al., 2006]. Physical parameters follow those set in the first experiment with the VUV photons [Wabnitz et al., 2002, Wabnitz, 2003].

(i) **Single photoionizations of atoms**. A single VUV photon of energy, $E_\gamma = 12.7$ eV, may excite electrons only from the $5p_{3/2}$ shell of xenon atoms of the binding energy, $E_i = 12.1$ eV. We neglect possible multistep photo- and multiphoton ionizations within this primary model. We also neglect the effect of plasma screening on the atomic energy levels and photoionization cross sections.

(ii) **Elastic and inelastic collisions of electrons with atoms/ions**. We assume that an inelastic collision always releases a secondary electron. We neglect inelastic collisions of electrons and atoms/ions which lead only to an excitation of an atom/ion. These processes contribute to the multistep collisional ionization which is not included within this primary model. We also neglect the effect of plasma screening on the collisional cross sections.

(iii) **Inverse bremsstrahlung photoabsorption in the presence of atoms or ions**. In our model, as the primary kinetic energy of a photoelectron released by a VUV photon is small, $E \sim 0.6$ eV, comparing to the first ionization energy, $E_i = 12.1$ eV, a process of energy pumping is necessary in order to initiate any collisional ionizations by electrons. Inverse bremsstrahlung process is among the possible processes [Santra & Greene, 2003]. At the low photoelectron energies, that we consider here, the proper description of the inverse bremsstrahlung should be quantum and not classical [Pert, 1996, Brantov et al., 2003]. Quantum cross sections for absorption or emission of radiation photons by electrons during their collisions with ions were taken from Ref. [Kroll & Watson, 1973]. In this approxima-

tion ions were treated as point-like charges [Kroll & Watson, 1973]. We have also calculated the quantum cross-section for inverse bremsstrahlung using the modified atomic potential including the spatial distribution of charge within an atom/ion. This treatment was proposed by Santra and Greene in [Santra & Greene, 2003]. In both cases we neglected the effect of plasma screening on the atomic/ionic potentials.

(iv) **Electromagnetic interaction of electrons with laser field**. Here this interaction is treated within the dipole approximation. This approach is justified by the small spatial size of the irradiated spherical cluster of a radius ~ 25 Å, when compared to the wavelength of laser radiation (~ 100 nm). We expect that the attenuation of the laser beam is small. Rough calculation of the attenuation via photoabsorption at the beginning of the pulse gives the transmission of about 94%. After all atoms have been photoionized, photons from the pulse can be still absorbed via inverse bremsstrahlung. Estimated total energy absorbed by this xenon cluster is about 300 keV at most.

(v) **Electromagnetic interactions of electrons and ions within the sample**. They are expressed in the form of the non-local potentials resulting from the solution of Poisson equation.

Finally, we note that within this primary model we also neglect the recoil energies and the recoil momenta of atoms/ions gained during their interactions with photons or electrons. Electrons are assumed to scatter isotropically on atoms/ions. This is the first order approximation which can be made: (i) in case of photoionizations due to the low energy of the incoming photons, and (ii) in case of collisional interactions due to the large difference of electron and ion masses and to the low impact energies of electrons. Within this approximation the movement of ions will be stimulated by the Coulomb repulsion only. Additional pressure on ions due to the recoil momenta is neglected.

Recoil effects, and also short-range electron-electron interaction can be conveniently treated by the means of the Fokker-Planck equation. As other relevant processes which were neglected within this primary model, e.g. three-body recombination, charge enhanced ionization [Siedschlag & Rost, 2004] or effects of electron screening [Santra & Greene, 2003], these processes will be treated in forthcoming papers.

3 Electron and ion dynamics inside an irradiated xenon cluster

We have formulated and solved numerically Boltzmann equations for a xenon cluster irradiated with VUV FEL photons. We followed the scheme presented in [Ziaja et al., 2006]. The following improvements have been made.

First, we enabled electron heating by including the inverse bremsstrahlung process. As we will later see, this process will lead to subsequent collisional ionizations inside the cluster. We consider two different inverse bremsstrahlung heating rates: (i) that one obtained with the assumption of point-like ions [Kroll & Watson, 1973] (slow heating), (ii) that one obtained with modified atomic potentials including the effect of spatial distribution of charge within ions [Santra & Greene, 2003] (fast heating). We will show that higher ionizations up to +8 inside the cluster can be obtained only in case of fast heating.

Second, we follow here the dynamics of both electrons and ions, i. e. ions are not longer frozen during the exposure as in Eq. [11] in [Ziaja et al., 2006]. They were now treated in the radial approximation:

$$\rho^i(\mathbf{r},\mathbf{v},t) \cong \rho_0^i(r,v,t)\,\delta(\,cos(\theta_{rv})-1\,). \tag{3}$$

Our initial configuration was given by a smooth atomic density function, representing a spherically symmetric cluster consisting of 1500 neutral xenon atoms. Edges of this sample were smoothed in order to facilitate computation. The density in the center was comparable to that of the xenon cluster, ~ 0.005 1/Å^3. The radius of this cluster was ~ 25 Å. This sample was irradiated with the VUV FEL photons of energies, $E_\gamma = 12.7$ eV. We have assumed that the photon pulse had a gaussian intensity shape, with a maximum at $I = 3 \cdot 10^{13}$ W/cm^2 and full width at half maximum, $\Delta t = 50$ fs (Fig. 1). This pulse intensity corresponded to an upper estimate of the maximal FEL pulse intensity observed in the experiment [Wabnitz et al., 2002].

We have solved the extended equations numerically with our Boltzmann solver. The simulation box had the size: ($0 < r < 100$ Å)$\times$ ($0 < v < 80$ Å/fs), and it was divided into 50$\times$64 grid points respectively. We followed the evolution of this system up to 300 fs of the exposure (Fig. 1). As in the previous study case, we followed the evolution of irradiated cluster, recording electron and ion densities at different times of the exposure (not shown). With these observables we estimated global parameters of the system as functions of time. Here we show: (a) electron temperature and (b) total number of electrons and ions of different charges created within the sample (Figs. 2,3). In Fig. 4 we also plot the histograms

of relative number of ions of different charges recorded at 300 fs compared to those obtained in the experiment [Wabnitz et al., 2002, Wabnitz, 2003].

In our extended model electrons gained energy via the inverse bremsstrahlung process. This effect is reflected in the shapes of the temperature curves (Figs. 2a,3a). The temperature of electrons increased with time until ~ 90 fs (Fig. 2a) and ~ 120 fs of the exposure (Fig. 3a). When the heating rate was fast, after this time many electrons were energetic enough to leave the simulation box (Fig. 2b) and the temperature of electrons within the box decreased. When the heating rate was slow, electrons did not gain enough energy to leave the cluster. They stayed inside the cluster, and thermalized (Fig. 3b).

Heating effiency was also reflected by the number of highly charged ions created within the irradiated sample. In case of fast heating, highly charged ions (up to +8) were created early in the exposure (up to ~ 80 fs). In case of slower heating, only ions of charges up to +3 could be created within the sample. Slow electrons stayed inside the sample kept by the Coulomb attracting potential. At the end of the laser pulse this electron-ion system reached an semi-equilibrium state.

At the time, $t = 300$ fs, there were no neutral atoms left within the cluster. Contributions of ions of specific charges to the total number of ions were following. In case of fast heating (Fig. 4a): Xe +1 ($\sim 20\%$), Xe +2 ($\sim 15\%$), Xe +3 ($\sim 15\%$), Xe +4 ($\sim 7.5\%$), Xe +5 ($\sim 7.5\%$), Xe +6 ($\sim 11\%$), Xe +7 ($\sim 11\%$) and Xe +8 ($\sim 13\%$), and the contribution of Xe +1 ions was the largest one. In case of slow heating (Fig. 4b), Xe +1 ($\sim 42\%$), Xe +2 ($\sim 56\%$) and Xe +3 ($\sim 2\%$), and the contribution of Xe +2 ions was the largest one.

In order to conclude, we note that from the above two IB models only the fast heating model, using quantum cross-sections obtained with the modified atomic potential, lead to the creation of highly charged ions up to +8 within the sample. Following results of Ref. [Santra & Greene, 2003] and our results, we would recommend to use this model for simulations of charge dynamics inside xenon clusters.

Summary and conclusions.

We have formulated general Boltzmann equations describing the evolution of a non-uniform sample irradiated with VUV FEL photons. We have solved these equations numerically with a dedicated algorithm. Two study cases including: (i) fast and (ii) slow electron heating rates were considered. They lead to different evolution scenarios.

In case when the heating was fast, highly charged ions up to +8 were created early in the

exposure. Many electrons gained energy sufficient to leave the ion cluster. As a result the outer shell of the cluster became positively charged.

In case when heating rate was slow, highly charged ions up to +3 were created. Only a small fraction of electrons could leave the sample. The majority of electrons stayed inside the cluster kept by the Coulomb attraction forces. At the end of the laser pulse this electron-ion system reached an semi-equilibrium state.

The results obtained with the extended model are promising. We observe a qualitative agreement between the charge densities and the average energy absorbed per atom estimated with this primary model and the experimental data. In the first experiments [Wabnitz et al., 2002] at a power density in the range 10^{13}- 10^{14} W/cm^2 charge states up to 8+ where observed. The estimated average energy absorbed per atom varied between 100 eV and 2500 eV, depending on the charge state. These numbers are in the same range as the values predicted in the present work. However, at this stage we can make only qualitative comparison of our predictions to the data. The model developed here needs further improvements of its physical assumptions in order to be applied to a realistic case. Effects of plasma screening on atomic energy levels and on photo- and collisional ionization cross sections have to be treated [Santra & Greene, 2003, Siedschlag & Rost, 2004]. So far potentials used in equations were unscreened, and cross sections (also inverse bremstrahlung cross sections) were also obtained with those unscreened potentials. Including the screening effects within this non-uniform sample can significantly affect the ionization dynamics. Important mechanisms of thermalization: recoil effects and short-range electron-electron interactions, need also to be treated in the improved model. Especially the latter effect will significantly change the distribution of energy among the plasma electrons and therefore also the ionization dynamics. Possible influence of recombination and of other many body processes on the sample dynamics requires dedicated analysis.

Only after treating all these effects, our model can be used for obtaining quantitative predictions.

We do not expect that including further interactions into these equations will lead to more numerical complicacies. As the main nonlinearity and stability problems have been successfully treated in the primary algorithm, and this algorithm correctly followed the dynamics of the sample in our study cases, we expect that it can easily be extended for a more advanced model.

At this point we have also to discuss the applicability of the classical approximation for describing the evolution of FEL irradiated samples (see also [Last & Jortner, 2006]). We stress here that our final aim is to obtain a description of radiation damage at short wave-

lenghts of photon radiation (soft and hard X-rays), when plasma electrons plasma are hot, and their treatment with classical Boltzmann equations therefore justified. When we try to apply the classical description to a sample irradiated with VUV FEL photons of $\lambda \sim 100$ nm ($E_\gamma = 12.7$ eV), and estimate the degeneracy parameter $\Upsilon = E_{Fermi}/k_B T$ for electrons, it is ~ 1 for electron plasma of temperature, $T \sim 1$ eV and density $n_e \sim 10^{22} cm^{-3}$, and it is ~ 20 for the plasma of the same temperature and density $n_e \sim 10^{24} cm^{-3}$ These values are much above the classical regime, $\Upsilon \ll 1$.

However, the evolution of an irradiated sample is a non-equilibrium process, and if the energy gain by electrons and electron escape rate from the sample were fast enough, the system could enter the classical regime very early in the exposure. Classical description could then still be applicable. This scenario is probable, according to the results obtained with our first study case. Therefore, in the realistic case it will be necessary to monitor the degeneracy parameters during the evolution of the sample. Their value will justify the validity of the classical approximation.

We believe that despite those limitations the method proposed here offers a unique possibility of studying the complex dynamics of large spatially non-uniform samples, irradiated with the FEL pulses. Whereas in real experiments the sample is exposed to several processes contributing simultaneously to the radiation damage, the Boltzmann simulation tool enables one to include specific interactions only. In this way the influence of different ionization mechanisms on the overall dynamics of the sample can conveniently be tested. Also, accurate time characteristics of damage processes can be obtained.

To sum up, Boltzmann approach is a first principle model which can follow non-equilibrium classical processes in phase space. Single particle densities evolved with Boltzmann equations include the full information on particle positions and velocites, and not only on their collective components. Average observables obtained with the Boltzman solver are not biased with statistical errors. However, the information on the three and higher order correlations is not included within Boltzmann equations. Including the effects of many body correlations into these classical equations is generally not possible, only in a few cases and under simplifying assumptions, e.g. by applying the Fokker-Planck equation in case of long-range Coulomb forces. The other serious disadvantage of the Boltzmann approach is its numerical complexity which requires an application of advanced numerical methods.

Computational costs within Boltzmann approach do not scale with the number of atoms within a sample, as in the MC method. Therefore, a Boltzmann solver is usually much more efficient for larger samples of a regular structure than a Monte Carlo code. This does not apply for samples of a complex or irregular structure. As these samples cannot be accurately represented by a smooth density function, Boltzmann equations can only give a crude esti-

mate of their damage dynamics. Improving the accuracy within the Boltzmann approach is possible only by extending the number of grid points used to represent the sample. This may lead to very long computational times when a large number of grid points was applied.

To sum up, we have demonstrated that the Boltzmann equations are a useful method to follow the radiation damage of non-uniform samples irradiated with the FEL photons. We believe that these equations may soon become a standard tool for investigating the complex dynamics of irradiated samples.

Acknowledgements

This research was supported in part by the Polish Committee for Scientific Research with grant No. 2 P03B 02724 and by the German Bundesministerium für Bildung und Forschung with grant No. 05 KS4 KTC/1. Beata Ziaja was a fellow of the Alexander von Humboldt Foundation.

References

[Bauer, 2004] Bauer, D. 2004. *J. Phys. B*, **37**, 3085.

[Brantov et al., 2003] Brantov, A., Rozmus, W., Sydora, R., Capjack, C. E., Bychenkov, V. Yu., & Tikhonchuk, V. T. 2003. *Physics of Plasmas*, **10**, 3385.

[Dattoli et al., 2005] Dattoli, G., Ottaviani, P. L., & Renieri, A. 2005. *Laser and Particle Beams*, **23**, 303–307.

[Chapman & Cowling, 1970] Chapman, S., & Cowling, T. G. 1970. The mathematical theory of non-uniform gases. *Cambridge Univerisy Press*.

[DESY, 2001] DESY. 2001. *TESLA, the Superconducting Electron-Positron Linear Collider with an integrated X-ray Laser Laboratory. Technical Design Report., DESY, ISBN 3-935702-00-0*, **5**, 150–168.

[DESY, 2006] DESY. 2006. *Technical Design Report of the European XFEL, DESY, ISBN 3-935702-17-5*, **5**, 7–9.

[Ditmire et al., 1996] Ditmire, T., Donnelly, T., Rubenchik, A. M., Falcone, R. W. & Perry, M. D. 1996. *Physical Review A*, **53**, 3379.

[Fisher et al., 2006] Fisher, D., Henis, Z., Eliezer, S., & Meyer-ter-Vehn, J. 2006. *Laser and Particle Beams*, **24**, 81–94.

[Hau-Riege et al., 2004] Hau-Riege, S. P., London, R. A., & Szöke, A. 2004. *Phys. Rev. E*, **69**, 051906.

[Heidenreich et al., 2005] Heidenreich, A., Last, I., & Jortner, J. 2005. *Eur. Phys. J. D*, **35**, 567.

[Jungreuthmayer et al., 2005] Jungreuthmayer, C., Ramunno, L., Zanghellini, J., & Brabec, T. 2005. *J. Phys. B*, **38**, 3029.

[Jurek et al., 2004] Jurek, Z., Faigel, G., & Tegze, M. 2004. *Eur. Phys. D*, **29**, 217.

[Kanapathipillai, 2006] Kanapathipillai, M. 2006. *Laser and Particle Beams*, **24**, 9–14.

[Krainov & Smirnov, 2002] Krainov, V. P., & Smirnov, M. B. 2002. *Phys. Rep.*, **370**, 237.

[Krenz & J. Meyer-ter-Vehn, 2005] Krenz, A., & J. Meyer-ter-Vehn. 2005. *Eur. Phys. D*, **36**, 199.

[Kroll & Watson, 1973] Kroll, N. M., & Watson, K. M. 1973. *Phys. Rev. A*, **8**, 804.

[Kruer, 1988] Kruer, W. L. 1988. The physics of laser plasma interactions. *Addison Wesley Publishing Company, Inc.*

[Last & Jortner, 1999] Last, I., & Jortner, J. 1999. *Phys. Rev. A*, **60**, 2215.

[Last & Jortner, 2006] Last, I., & Jortner, J. 2006. *Phys. Rev. A*, **73**, 013202.

[LCLS, 2000] LCLS. 2000. *LCLS: The First Experiments., SSRL, SLAC, Stanford, USA.*

[Lee at el., 2002] Lee, R. W., Baldis, H. A., Cauble, R. C., Landen, O. L., Wark, J. S., Ng, A., Rose, S. J., Lewis, C., Riley, D., Gauthier, J. C., & Audebert, P. 2002. *Laser and Particle Beams*, **20**, 527–536.

[Meyer-ter-Vehn et al., 2004] Meyer-ter-Vehn, J., Krenz, A., Ke Lan, Eidmann, K., Fill, E., Rosmej, F., Schlegel, Th., Sokolowski-Tinten, K., von der Linde, D. & Tschentscher Th. 2004. Dense plasma studied with XFELs. *Inertial Fusion Sciences and Applications (eds. B. A. Hammel et al.), American Nuclear Society, La Grange Park, Illinois*, 912–916.

[Neutze et al., 2000] Neutze, R., Wouts, R., van der Spoel, D., Weckert, E., & Hajdu, J. 2000. *Nature*, **406**, 752–757.

[Pert, 1996] Pert, G. J. 1996. *J. Phys. B*, **29**, 1135.

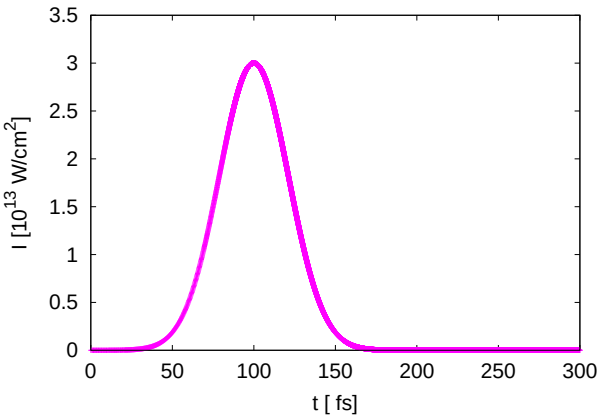

Figure 1: Intensity of the pulse as function of time.

[Saalmann & Rost, 2002] Saalmann, U., & Rost, J.-M. 2002. *Phys. Rev. Lett.*, **89**, 143401.

[Saalmann et al., 2006] Saalmann, U., Siedschlag, C., & Rost, J. M. 2006. *J. Phys. B*, **39**, R39.

[Santra & Greene, 2003] Santra, R., & Greene, C. H. 2003. *Phys. Rev. Lett.*, **91**, 233401.

[SCSS, 2006] Shintake, T., & SCSS Team *Status of Japanese XFEL Project and SCSS test accelerator*, *Proceedings of FEL 2006, BESSY, Berlin, Germany*, 33-36.

[Sharkofsky et al., 1966] Sharkofsky, I. P., Johnston, T. W., & Bachynski, M. P. 1966. The particle kinetics of plasmas. *Addison Wesley Publishing Company, Inc.*

[Siedschlag & Rost, 2004] Siedschlag, C., & Rost, J.M. 2004. *Phys. Rev. Lett.*, **93**, 043402.

[Wabnitz et al., 2002] Wabnitz, H., Bittner, L., de Castro, A. R. B., Döhrmann, R., Gürtler, P., Laarmann, T., Laasch, W., Schulz, J., Swiderski, A., von Haeften, K., Möller, T., Faatz, B., Fateev, A., Feldhaus, J., Gerth, C., Hahn, U., Saldin, E., Schneidmiller, E., Sytchev, K., Tiedtke, K., Treusch, R., & Yurkov M. 2002. *Nature*, **420**, 482.

[Wabnitz, 2003] Wabnitz, H. 2003. Interaction of intense VUV radiation from FEL with rare gas atoms and clusters. *Doctoral Thesis*, *DESY-THESIS-2003-026*.

[Ziaja et al., 2006] Ziaja, B., de Castro, A. R. B., Weckert, E., & Möller, T. 2006. *Eur. Phys. J. D*, **40**, 465.

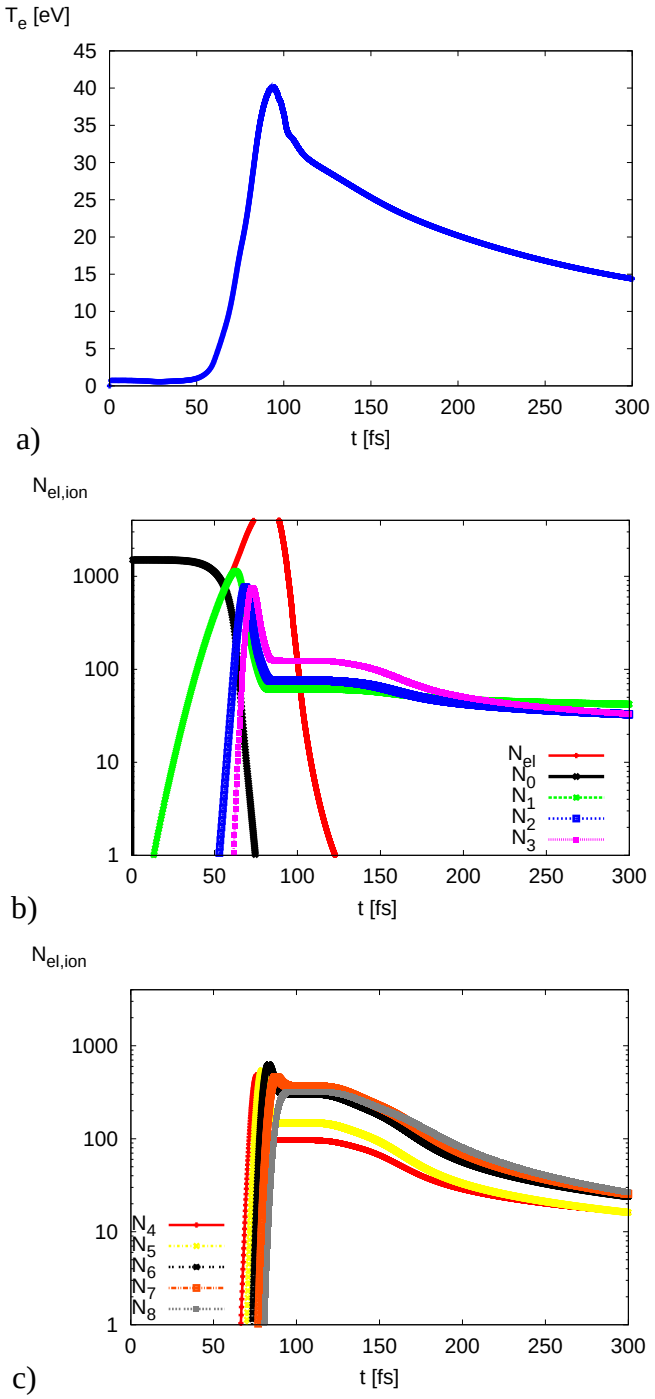

Figure 2: Global parameters of the irradiated sample as function of time: a) electron temperature, b-c) number of electrons and ions created within the sample: b) ions up to +3, c) ions from +4 up to +8. These results were obtained in case of the irradiation with the VUV FEL photons of energies, $E_\gamma = 12.7$ eV, when the quantum cross section for the inverse bremsstrahlung was calculated with modified atomic potentials as in Ref. [Santra & Greene, 2003].

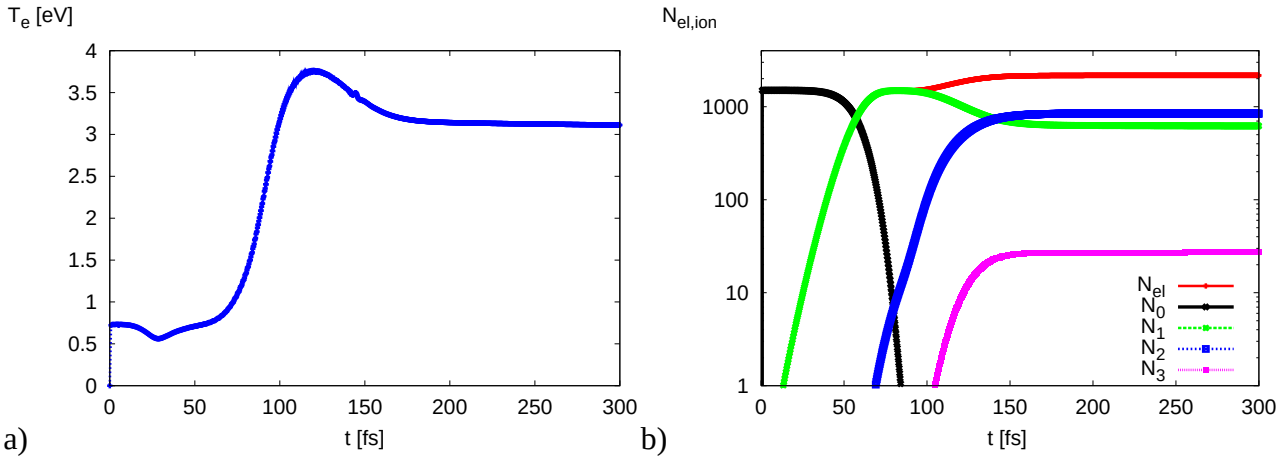

Figure 3: Global parameters of the irradiated sample as function of time: a) electron temperature, b) number of electrons and ions created within the sample: ions up to +3. Ions of higher charges were not observed. These results were obtained in case of the irradiation with the VUV FEL photons of energies, $E_\gamma = 12.7$ eV, when the quantum cross section for the inverse bremsstrahlung was calculated for point-like ions as in Ref. [Kroll & Watson, 1973].

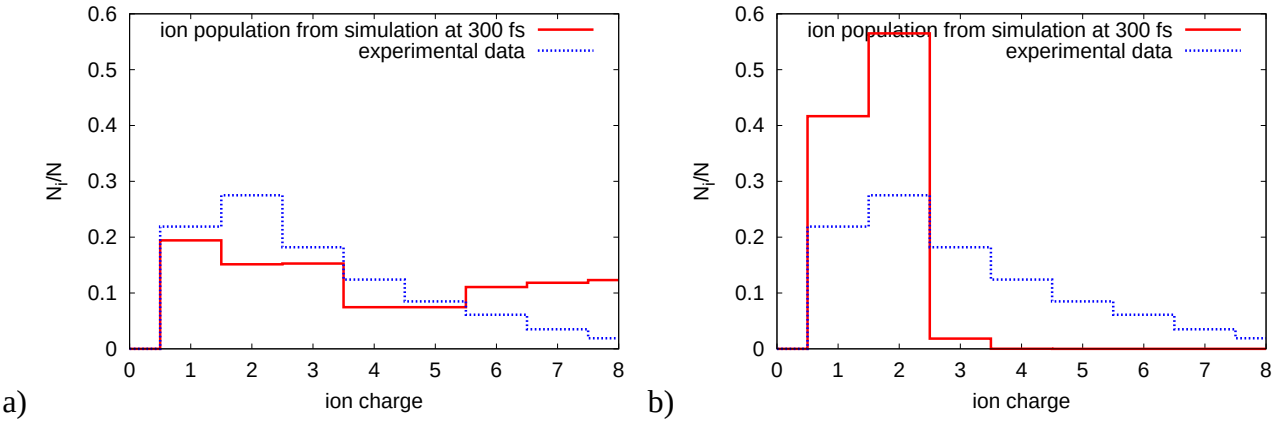

Figure 4: Histograms of the relative number of ions of different charges, N_i/N, recorded at 300 fs, compared to those obtained in the experiment [Wabnitz et al., 2002, Wabnitz, 2003]. Predictions from our simulation were obtained in case of the irradiation with the VUV FEL photons of energies, $E_\gamma = 12.7$ eV, when: a) the quantum cross section for the inverse bremsstrahlung was calculated with modified atomic potentials, and b) the quantum cross section for the inverse bremsstrahlung was calculated for point-like ions [Kroll & Watson, 1973].